GSA Data Repository 2018059

Liu et al., 2018, Limited recycling of crustal osmium in forearc mantle during slab dehydration: Geology, https://doi.org/10.1130/G39869.1.

# SUPPLEMENTARY MATERIALS

## Supplementary text:

***1. Sample description***

***2. Analytical methodology***

**Fig. DR1:** Scanned thin-section images of New Caledonia peridotites

**Fig. DR2:** Microtextures of New Caledonia peridotites

**Fig. DR3:** Whole rock CaO vs $Al_2O_3$.

**Fig. DR4:** $^{187}Os/^{188}Os$ vs $^{187}Re/^{188}Os$ (a) and $Al_2O_3$ contents (b).

**Table DR1:** Whole rock and mineral major element compositions of the New Caledonia peridotites

**Table DR2:** Whole rock Re-Os isotope compositions of the New Caledonia peridotites

## Supplementary text

### 1. Sample description

Mantle peridotites from the New Caledonia ophiolites selected in this study include ten lherzolites from the Tiebaghi massif (20°22'43" S, 164°7'12" E) and thirty-four harzburgites from three massifs, including nine samples from Ouassë Bay (21°27'31" S, 166°2'8" E), twenty samples from Me Maoya (21°28'3" S, 165°23'40" E) and five samples from Massif du Sud (22°13'28" S, 166°37'38" E). Most of them are highly serpentinized (Fig. DR1a, b), and very fresh samples were only collected from the Me Maoya massif (Fig. DR1c, d). They mainly display a porphyroclastic texture (Fig. DR1a, c), in which orthopyroxene occurs as the phorphyroclast and olivine was variably recrystallized. Deformed textures can be observed in some samples, in which either orthopyroxene or olivine has been strongly elongated (Fig. DR1b, d). Olivines in the deformed peridotites are locally mylonitized (Fig. DR1d).

The serpentinized peridotites display a typical mesh-like texture, in which olivine is replaced or crosscut by serpentine minerals (Fig. DR2a, b). Spinel commonly displays a lobate shape. Tiny spinels are disseminated within the serpentines or occur at the rim of orthopyroxene porphyroclasts. In the fresh samples, olivine porphyroclasts have well-developed kink bands (Fig. DR2c, d). Triple junctions are locally preserved in the fresh samples (Fig. DR2d). Orthopyroxenes are the main porphyroclasts and display well-developed exsolution lamellae (Fig. DR2e, f). They commonly have irregular boundaries and are surrounded or replaced by olivine neoblasts. Clinopyroxenes occur as neoblasts among olivines or orthopyroxenes (Fig.

DR2e).

## 2. Analytical methodology

### *2.1. Whole rock and mineral major elements*

Major elements were analysed using X-ray fluorescence (XRF) at the Institute of Geology and Geophysics, Chinese Academy of Sciences (IGGCAS). About 0.5 g of sample powders were weighted and mixed with 5 g of $Li_2B_4O_7$ to make glass beads. Before making the beads, loss on ignition (LOI) were obtained by the weight difference before and after high temperature of 1000°C calcinations. The glass beads were analyzed on an AXIOS Mineral Spectrometer, with analytical uncertainties for major elements varying from 1% to 3%.

Mineral major elements were analyzed by wavelength-dispersive spectrometry (WDS) on a JEOL JXA-8100 electron probe, with an accelerating voltage of 15 kV and a beam current of 20 nA. Natural minerals and synthetic oxides were used as standards, and the ZAF procedure was used for matrix corrections.

### *2.2. Re-Os isotopes*

Whole rock Re-Os isotopes were analyzed by isotope dilution method, following the procedure previously described (Chu et al., 2009). About 2g of powder, together with Re-Os (i.e., $^{187}Re$ and $^{190}Os$) and HSE ($^{99}Ru$, $^{105}Pd$, $^{191}Ir$ and $^{194}Pt$) isotope tracers, was digested with reverse aqua regia (i.e., 3 ml 12N HCl and 6 ml 16N $HNO_3$) in a Carius Tube at 240 $^{o}$C for ca. 48-72 hours. Osmium was extracted from the aqua regia solution by solvent extraction into $CCl_4$ and further purified by micro-distillation (Birck et al., 1997). Afterwards, Ru, Pd, Re, Ir and Pt were sequentially separated from the solution by anion exchange resin (AG-1×8, 100-200 mesh).

Osmium isotopes were measured by N-TIMS on a GV Isoprobe-T instrument in a static mode using Faraday cups. To increase the ionization efficiency, $Ba(OH)_2$ solution was used as an ion emitter. The measured Os isotopes were corrected for mass fractionation using the $^{192}Os/^{188}Os$ ratio of 3.0827. The Nier oxygen isotope composition ($^{17}O/^{16}O$=0.0003708 and $^{18}O/^{16}O$=0.002045) has been used for oxide correction. The in-run precisions for Os isotopic measurements were better than 0.2% (2σ) for all the samples. Johnson-Matthey standard of UMD was used as an external standard, yielding a $^{187}Os/^{188}Os$ ratio of 0.11378±2 (2 δ; n=5). The Re content was measured on a Neptune MC-ICPMS using an electron multiplier in a peak-jumping mode or using Faraday cups in a static mode, according to the measured signal intensity. Iridium was added as an external standard to correct mass fractionation of Re and in-run precision for $^{185}Re/^{187}Re$ was ~ 0.1-0.3% (2 δ). The total procedural Os blank has a content of 3±1 pg (n=4) and a $^{187}Os/^{188}Os$ ratio of ~ 0.15, and the total procedural blank for Re was 4±2 pg (n=4). Three standards, i.e., WPR-1, UB-N and BHVO-2, were analysed as unknowns in analytical sessions. The WPR-1 yields 11.19 ppb Re, 16.96 ppb Os, and a $^{187}Os/^{188}Os$ ratio of 0.14451±0.00013, which is 0.57 ppb, 0.08 ppb and 0.15560±0.00043 for BHVO-2, respectively. Our results are consistent with the published values (Day et al., 2016; Li et al., 2015). Moreover, the obtained Re-Os contents (i.e., 0.22 ppb and 3.54 ppb, respectively) and $^{187}Os/^{188}Os$ ratio (0.12726±0.00016) of UB-N are identical to the published values within errors (Ishikawa et al., 2014).

## References

Birck, J.-L., Roy-Barman, M., and Capmas, F., 1997, Re-Os isotopic measurements at the femtomole level in natural samples: Geostandards and Geoanalytical Research, v. 21, no. 1, p. 19-27.

Chu, Z. Y., Wu, F. Y., Walker, R. J., Rudnick, R. L., Pitcher, L., Puchtel, I. S., Yang, Y. H., and Wilde, S. A., 2009, Temporal evolution of the lithospheric mantle beneath the eastern North China Craton: Journal of Petrology, v. 50, p. 1857-1898.

Day, J. M. D., Walters, C. L., Shaefer, B. F., Walker, R. J., and Turner, S., 2016, Use of hydrofluoric ccid desilicification in the determination of highly siderophile element abundances and Re-Pt-Os isotope systematics in mafic-ultramafic rocks: Geostandards and Geoanalytical Research, v. 40, p. 49-65.

Ishikawa, A., Senda, R., Suzuki, K., Dale, C. W., and Meisel, T., 2014, Re-evaluating digestion methods for highly siderophile element and $^{187}Os$ isotope analysis: Evidence from geological reference materials: Chemical Geology, v. 384, p. 27-46.

Li, J., Zhao, P. P., Liu, J. G., Wang, X. C., Yang, Y. A., Wang, G. Q., and Xu, J. F., 2015, Reassessment of hydrofluoric acid desilicification in the Carius Tube digestion technique for Re-Os isotopic determination in geological samples: Geostandards and Geoanalytical Research, v. 39, p. 17-30.

**Fig. DR1: Scanned thin-section images of New Caledonia peridotites**

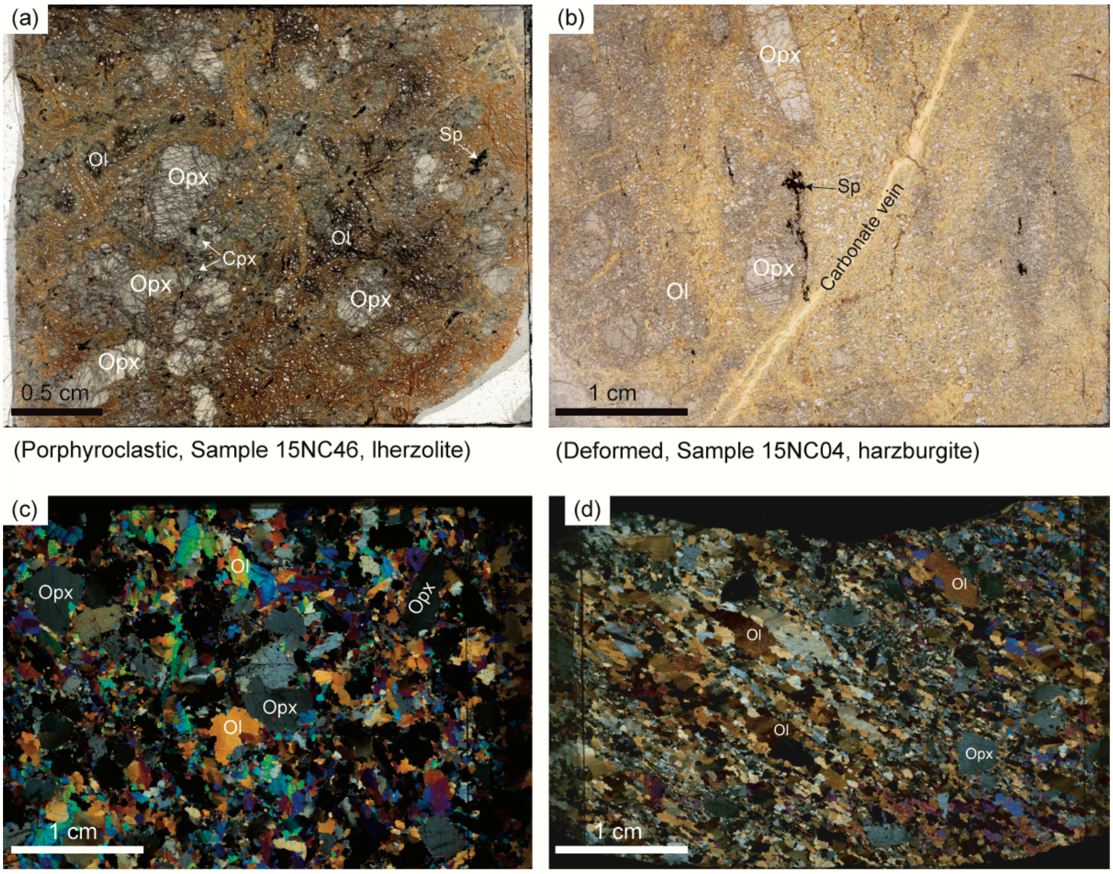


(Porphyroclastic, Sample 15NC46, lherzolite) (Deformed, Sample 15NC04, harzburgite)

(Porphyroclastic, Sample 15NC20, harzburgite) (Deformed, Sample 15NC25, harzburgite)

**Fig. DR2: Microtextures of New Caledonia peridotites**

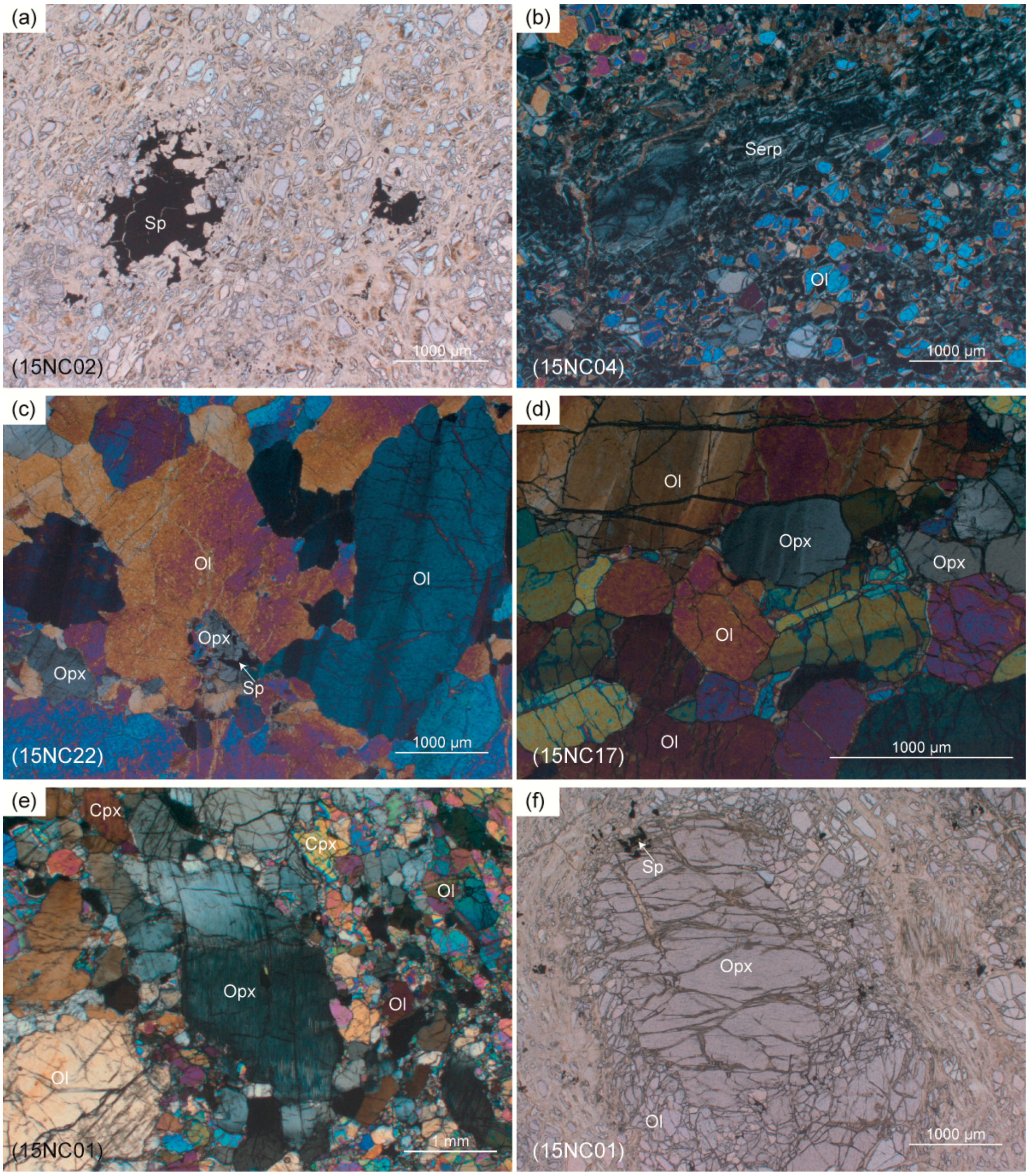

**Fig. DR3: Whole rock CaO vs $Al_2O_3$. Data for abyssal peridotites are compiled from PetDB (http://www.earthchem.org/petdb).**

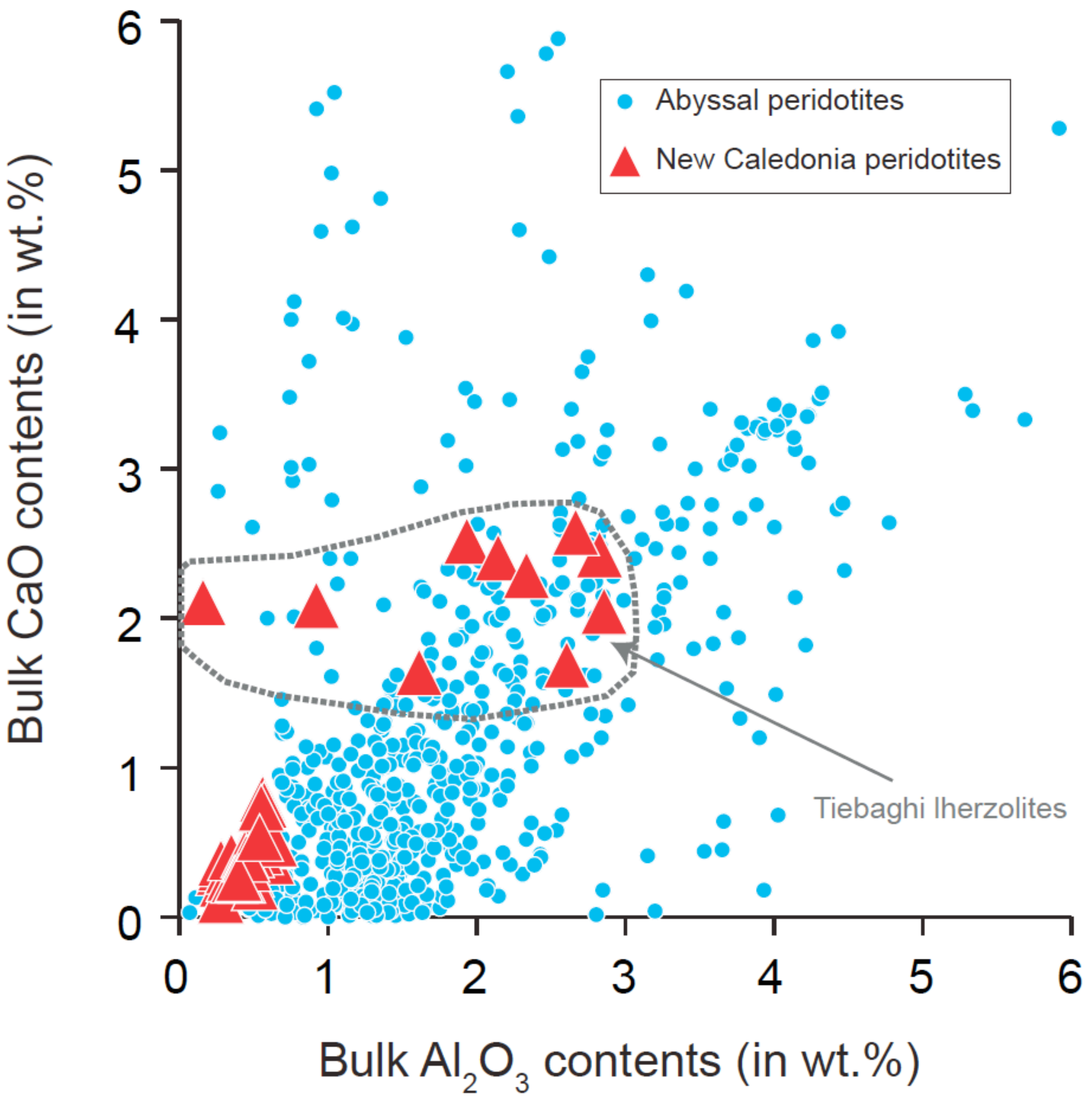

**Fig. DR4: $^{187}Os/^{188}Os$ vs $^{187}Re/^{188}Os$ (a) and $Al_2O_3$ contents (b).**

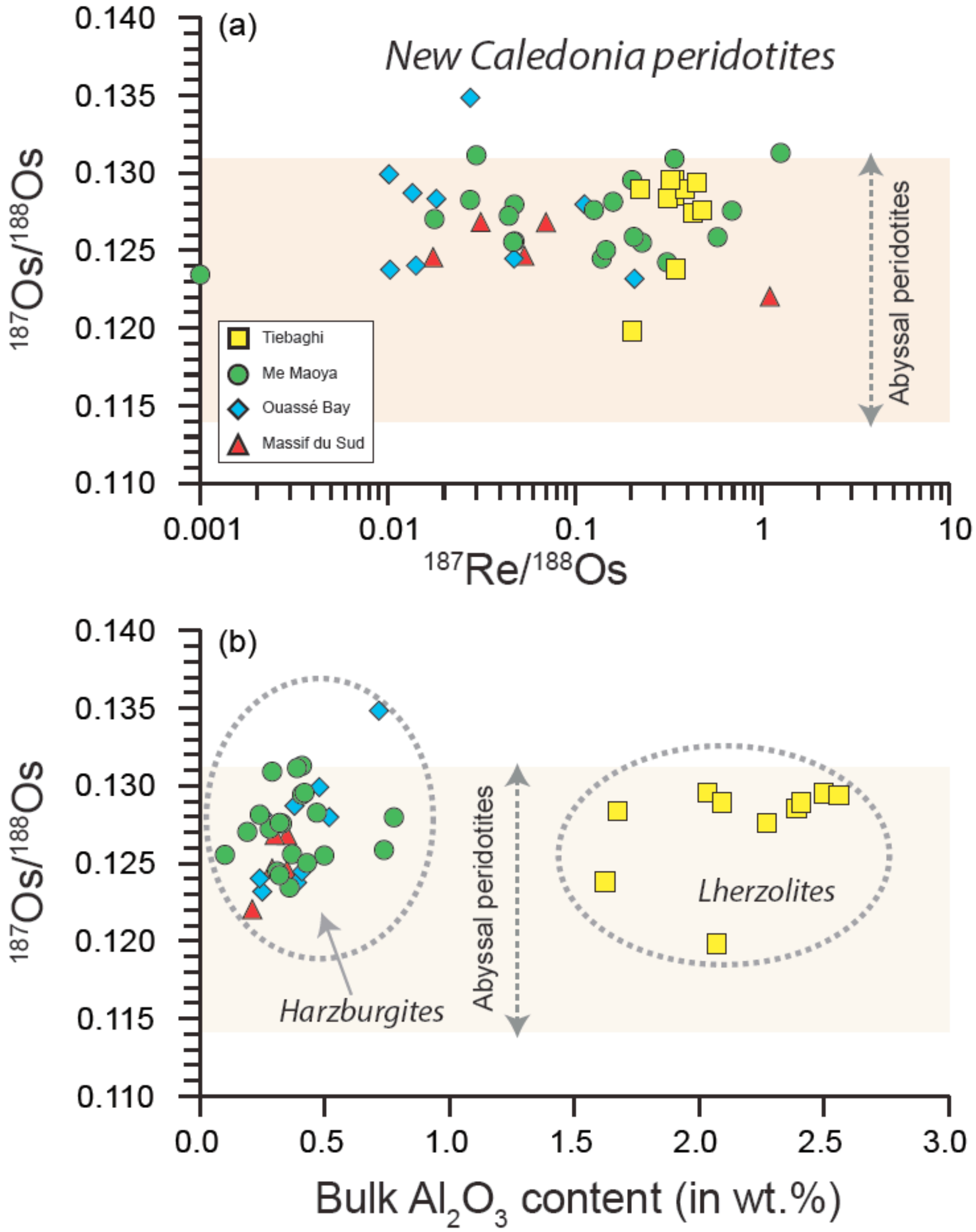

**Table DR1-Major elements of the New Caledonia peridotites**

| Sample | Locality | Litho. | $SiO_2$ | $TiO_2$ | $Al_2O_3$ | $Cr_2O_3$ | $TFe_2O_3$ | MnO | MgO | CaO | $Na_2O$ | $K_2O$ | NiO | LOI | Total | Ol Fo | Sp Mg# | Sp Cr# | Sp $TiO_2$ |
|---|---|---|---|---|---|---|---|---|---|---|---|---|---|---|---|---|---|---|---|
| 15NC01 | | Hazb. | 40.02 | 0.00 | 0.52 | 0.34 | 7.68 | 0.11 | 41.35 | 0.48 | 0.00 | 0.00 | 0.29 | 9.49 | 100.28 | 0.91 | 0.48 | 0.65 | 0.01 |
| 15NC02 | | Hazb. | 42.08 | 0.00 | 0.72 | 0.38 | 7.61 | 0.11 | 40.75 | 0.49 | 0.00 | 0.00 | 0.29 | 7.90 | 100.33 | 0.91 | 0.46 | 0.63 | 0.01 |
| 15NC03 | | Hazb. | 41.48 | 0.01 | 0.25 | 0.35 | 7.90 | 0.11 | 41.21 | 0.34 | 0.00 | 0.00 | 0.31 | 7.91 | 99.88 | 0.91 | 0.53 | 0.66 | 0.00 |
| 15NC04 | | Hazb. | 41.11 | 0.00 | 0.38 | 0.53 | 7.90 | 0.11 | 41.41 | 0.39 | 0.00 | 0.00 | 0.29 | 8.22 | 100.34 | 0.91 | 0.45 | 0.65 | 0.01 |
| 15NC05 | Ouassë Bay | Hazb. | 41.03 | 0.00 | 0.24 | 0.25 | 7.85 | 0.11 | 41.56 | 0.31 | 0.00 | 0.00 | 0.30 | 8.65 | 100.31 | 0.91 | 0.50 | 0.67 | 0.01 |
| 15NC06 | | Hazb. | 41.13 | 0.01 | 0.48 | 0.42 | 8.47 | 0.12 | 40.67 | 0.58 | 0.00 | 0.00 | 0.30 | 7.78 | 99.96 | 0.91 | 0.57 | 0.56 | 0.04 |
| 15NC07 | | Hazb. | 41.67 | 0.00 | 0.41 | 0.42 | 7.84 | 0.11 | 39.99 | 0.38 | 0.00 | 0.02 | 0.30 | 8.91 | 100.05 | 0.91 | 0.57 | 0.57 | 0.02 |
| 15NC08 | | Hazb. | 40.64 | 0.00 | 0.39 | 0.54 | 7.79 | 0.11 | 41.06 | 0.29 | 0.00 | 0.00 | 0.30 | 8.73 | 99.86 | 0.91 | 0.52 | 0.62 | 0.01 |
| 15NC09 | | Hazb. | 40.37 | 0.00 | 0.25 | 0.33 | 7.92 | 0.11 | 41.02 | 0.28 | 0.00 | 0.01 | 0.31 | 9.31 | 99.92 | 0.92 | 0.53 | 0.62 | 0.01 |
| 15NC11 | | Hazb. | 41.51 | 0.01 | 0.39 | 0.32 | 7.64 | 0.11 | 43.41 | 0.36 | 0.00 | 0.00 | 0.30 | 6.17 | 100.22 | 0.92 | 0.61 | 0.55 | 0.00 |
| 15NC12 | | Hazb. | 40.32 | 0.00 | 0.32 | 0.36 | 7.69 | 0.11 | 42.37 | 0.40 | 0.00 | 0.00 | 0.30 | 8.15 | 100.02 | 0.91 | 0.60 | 0.55 | 0.01 |
| 15NC13 | | Hazb. | 41.72 | 0.00 | 0.41 | 0.44 | 7.50 | 0.11 | 43.33 | 0.42 | 0.00 | 0.00 | 0.30 | 5.96 | 100.18 | 0.92 | 0.65 | 0.59 | 0.00 |
| 15NC15 | | Hazb. | 41.13 | 0.00 | 0.24 | 0.28 | 7.68 | 0.11 | 43.72 | 0.36 | 0.00 | 0.00 | 0.32 | 6.18 | 100.02 | 0.92 | 0.62 | 0.58 | 0.00 |
| 15NC17 | | Hazb. | 43.78 | 0.00 | 0.19 | 0.34 | 7.99 | 0.12 | 45.53 | 0.45 | 0.00 | 0.00 | 0.33 | 0.64 | 99.38 | 0.91 | 0.53 | 0.68 | 0.01 |
| 15NC20 | | Hazb. | 43.70 | 0.00 | 0.42 | 0.57 | 8.05 | 0.12 | 45.99 | 0.40 | 0.00 | 0.00 | 0.34 | 0.04 | 99.64 | 0.92 | 0.61 | 0.60 | 0.00 |
| 15NC21 | | Hazb. | 43.52 | 0.00 | 0.43 | 0.41 | 8.11 | 0.12 | 45.68 | 0.48 | 0.00 | 0.00 | 0.33 | 0.74 | 99.83 | 0.92 | 0.61 | 0.56 | 0.01 |
| 15NC22 | | Hazb. | 43.92 | 0.00 | 0.41 | 0.59 | 7.87 | 0.12 | 45.50 | 0.37 | 0.00 | 0.00 | 0.33 | -0.06 | 99.05 | 0.92 | 0.61 | 0.63 | 0.01 |
| 15NC23 | | Hazb. | 43.19 | 0.00 | 0.32 | 0.34 | 8.39 | 0.12 | 46.53 | 0.40 | 0.00 | 0.00 | 0.35 | 0.30 | 99.94 | 0.92 | 0.62 | 0.56 | 0.00 |
| 15NC24 | Me Maoya massif | Hazb. | 44.47 | 0.00 | 0.29 | 0.30 | 7.84 | 0.12 | 45.75 | 0.36 | 0.00 | 0.00 | 0.33 | 0.06 | 99.52 | 0.92 | 0.61 | 0.64 | 0.01 |
| 15NC25 | | Hazb. | 44.79 | 0.02 | 0.74 | 0.68 | 7.14 | 0.10 | 45.09 | 0.51 | 0.00 | 0.00 | 0.48 | 0.24 | 99.81 | 0.93 | 0.65 | 0.57 | 0.16 |
| 15NC26 | | Hazb. | 42.49 | 0.00 | 0.31 | 0.40 | 8.07 | 0.11 | 45.46 | 0.32 | 0.00 | 0.00 | 0.34 | 1.88 | 99.38 | 0.92 | 0.58 | 0.59 | 0.01 |
| 15NC27 | | Hazb. | 43.05 | 0.00 | 0.47 | 0.39 | 8.12 | 0.12 | 43.40 | 0.56 | 0.00 | 0.00 | 0.31 | 3.58 | 99.99 | 0.91 | 0.60 | 0.55 | 0.01 |
| 15NC28 | | Hazb. | 43.52 | 0.00 | 0.28 | 0.37 | 8.13 | 0.12 | 45.09 | 0.42 | 0.00 | 0.00 | 0.33 | 1.36 | 99.63 | 0.91 | 0.60 | 0.66 | 0.01 |
| 15NC29 | | Hazb. | 43.66 | 0.00 | 0.36 | 0.40 | 8.30 | 0.12 | 45.29 | 0.56 | 0.00 | 0.00 | 0.33 | 0.28 | 99.31 | 0.91 | 0.58 | 0.59 | 0.00 |
| 15NC30 | | Hazb. | 44.85 | 0.00 | 0.78 | 1.10 | 7.30 | 0.11 | 44.45 | 0.50 | 0.00 | 0.00 | 0.35 | 0.10 | 99.54 | 0.92 | 0.61 | 0.59 | 0.01 |
| 15NC31 | | Hazb. | 42.54 | 0.00 | 0.10 | 0.33 | 8.36 | 0.12 | 45.24 | 0.22 | 0.00 | 0.00 | 0.33 | 2.46 | 99.70 | 0.91 | 0.46 | 0.72 | 0.03 |
| 15NC32 | | Hazb. | 44.25 | 0.01 | 0.33 | 0.38 | 7.76 | 0.11 | 45.87 | 0.34 | 0.00 | 0.00 | 0.33 | 0.02 | 99.39 | 0.92 | 0.58 | 0.62 | 0.05 |
| 15NC33 | | Hazb. | 44.06 | 0.00 | 0.50 | 0.50 | 7.98 | 0.12 | 44.84 | 0.42 | 0.00 | 0.00 | 0.34 | 0.82 | 99.57 | 0.92 | 0.62 | 0.56 | 0.01 |
| 15NC34 | | Hazb. | 43.85 | 0.00 | 0.37 | 0.34 | 8.19 | 0.12 | 45.42 | 0.49 | 0.00 | 0.00 | 0.33 | -0.02 | 99.10 | 0.91 | 0.62 | 0.57 | 0.01 |
| 15NC37 | | Lherz. | 39.24 | 0.03 | 2.10 | 0.35 | 8.41 | 0.09 | 35.45 | 0.10 | 0.10 | 0.03 | 0.35 | 13.75 | 100.02 | 0.90 | | | |
| 15NC38 | | Lherz. | 42.47 | 0.04 | 2.04 | 0.49 | 7.78 | 0.12 | 36.79 | 2.79 | 0.00 | 0.00 | 0.25 | 7.23 | 100.00 | | 0.54 | 0.50 | 0.25 |
| 15NC39 | | Lherz. | 41.35 | 0.05 | 2.57 | 0.39 | 7.97 | 0.12 | 35.72 | 2.60 | 0.00 | 0.01 | 0.24 | 8.65 | 99.67 | 0.90 | 0.53 | 0.49 | 0.35 |
| 15NC41 | | Lherz. | 42.04 | 0.04 | 2.28 | 0.35 | 8.30 | 0.12 | 37.53 | 2.27 | 0.00 | 0.01 | 0.26 | 6.63 | 99.83 | 0.90 | 0.53 | 0.50 | 0.37 |
| 15NC42 | Tiebaghi massif | Lherz. | 41.94 | 0.05 | 2.42 | 0.38 | 8.13 | 0.12 | 36.35 | 2.76 | 0.00 | 0.01 | 0.24 | 7.09 | 99.49 | 0.90 | 0.53 | 0.49 | 0.36 |
| 15NC43 | | Lherz. | 41.04 | 0.04 | 1.68 | 0.34 | 8.42 | 0.12 | 37.79 | 2.54 | 0.00 | 0.01 | 0.28 | 7.63 | 99.89 | 0.90 | 0.52 | 0.52 | 0.42 |
| 15NC44 | | Lherz. | 42.59 | 0.06 | 2.40 | 0.38 | 8.23 | 0.12 | 36.09 | 2.08 | 0.03 | 0.02 | 0.26 | 7.48 | 99.75 | 0.90 | 0.51 | 0.49 | 0.38 |
| 15NC45 | | Lherz. | 43.29 | 0.05 | 2.51 | 0.40 | 8.21 | 0.12 | 35.49 | 1.87 | 0.04 | 0.02 | 0.25 | 7.40 | 99.66 | 0.90 | 0.48 | 0.51 | 0.35 |
| 15NC46 | | Lherz. | 40.89 | 0.04 | 1.63 | 0.33 | 8.26 | 0.12 | 38.94 | 1.55 | 0.00 | 0.01 | 0.26 | 8.37 | 100.41 | 0.90 | 0.52 | 0.51 | 0.38 |
| 15NC48 | | Lherz. | 42.43 | 0.04 | 2.08 | 0.35 | 8.75 | 0.12 | 36.67 | 0.86 | 0.00 | 0.03 | 0.27 | 8.41 | 100.01 | 0.90 | 0.50 | 0.50 | 0.42 |

**Table DR1-Major elements of the New Caledonia peridotites**

| Sample | Locality | Litho. | $SiO_2$ | $TiO_2$ | $Al_2O_3$ | $Cr_2O_3$ | $TFe_2O_3$ | MnO | MgO | CaO | $Na_2O$ | $K_2O$ | NiO | LOI | Total | Ol Fo | Sp Mg# | Sp Cr# | Sp $TiO_2$ |
|---|---|---|---|---|---|---|---|---|---|---|---|---|---|---|---|---|---|---|---|
| 15NC84 | Massif du Sud | Hazb. | 40.51 | 0.00 | 0.30 | 0.42 | 7.55 | 0.11 | 42.67 | 0.27 | 0.00 | 0.01 | 0.30 | 8.06 | 100.21 | 0.92 | 0.53 | 0.71 | 0.01 |
| 15NC85 | | Hazb. | 40.77 | 0.01 | 0.35 | 0.41 | 7.22 | 0.10 | 43.02 | 0.22 | 0.00 | 0.01 | 0.30 | 8.05 | 100.47 | 0.92 | 0.62 | 0.69 | 0.01 |
| 15NC85-R | | Hazb. | 40.46 | 0.00 | 0.32 | 0.41 | 7.19 | 0.10 | 42.78 | 0.22 | 0.00 | 0.01 | 0.31 | 8.11 | 99.91 | | | | |
| 15NC86 | | Hazb. | 38.74 | 0.00 | 0.21 | 0.30 | 7.33 | 0.11 | 41.68 | 0.23 | 0.00 | 0.01 | 0.30 | 11.15 | 100.07 | 0.92 | 0.48 | 0.74 | 0.01 |
| 15NC87 | | Hazb. | 40.21 | 0.01 | 0.29 | 0.36 | 7.48 | 0.11 | 43.32 | 0.21 | 0.00 | 0.01 | 0.29 | 8.69 | 100.99 | 0.92 | 0.59 | 0.70 | 0.01 |
| 15NC88 | | Hazb. | 40.97 | 0.007 | 0.35 | 0.33 | 7.49 | 0.11 | 43.43 | 0.23 | 0.00 | 0.01 | 0.30 | 7.00 | 100.23 | 0.92 | 0.52 | 0.69 | 0.01 |

R: replicate analysis

Mg#=Mg/(Mg+$Fe^{2+}$)

Cr#=Cr/(Cr+Al)

**Table DR2-Whole rock Re-Os isotopes of the New Caledonia peridotites**

| Sample | Locality | Litho. | Re | Os | $^{187}Re/^{188}Os$ | $^{187}Os/^{188}Os$ | 2δ | $T_{MA}$ (Ga) | $T_{RD}$ (Ga) |
|---|---|---|---|---|---|---|---|---|---|
| WPR-1 | | S | 11.19 | 16.96 | 3.19 | 0.14451 | 0.00013 | | |
| UB-N | | S | 0.22 | 3.54 | 0.30 | 0.12726 | 0.00016 | | |
| BHVO-2 | | S | 0.57 | 0.08 | 34.79 | 0.15660 | 0.00043 | | |
| 15NC84 | Massif du Sud | H | 0.010 | 0.51 | 0.071 | 0.12688 | 0.00060 | 0.46 | 0.38 |
| 15NC85 | | H | 0.010 | 3.31 | 0.018 | 0.12463 | 0.00031 | 0.73 | 0.70 |
| 15NC86 | | H | 0.020 | 0.08 | 1.117 | 0.12211 | 0.00049 | -0.65 | 1.05 |
| 15NC87 | | H | 0.020 | 1.51 | 0.054 | 0.12473 | 0.00022 | 0.79 | 0.69 |
| 15NC88 | | H | 0.020 | 1.34 | 0.032 | 0.12689 | 0.00016 | 0.38 | 0.38 |
| 15NC01 | Ouassë Bay | H | 0.010 | 0.36 | 0.114 | 0.12803 | 0.00038 | 0.30 | 0.22 |
| 15NC02 | | H | 0.020 | 3.17 | 0.028 | 0.13486 | 0.00034 | -0.80 | -0.75 |
| 15NC03 | | H | 0.030 | 0.82 | 0.163 | 0.12817 | 0.00022 | 0.33 | 0.20 |
| 15NC04 | | H | 0.010 | 3.34 | 0.014 | 0.12875 | 0.00012 | 0.12 | 0.12 |
| 15NC04-R | | H | 0.010 | 1.33 | 0.018 | 0.12838 | 0.00021 | 0.18 | 0.17 |
| 15NC05 | | H | 0.010 | 2.79 | 0.014 | 0.12409 | 0.00019 | 0.80 | 0.78 |
| 15NC06 | | H | 0.010 | 4.14 | 0.010 | 0.12995 | 0.00021 | -0.05 | -0.05 |
| 15NC07 | | H | 0.020 | 2.14 | 0.048 | 0.12455 | 0.00014 | 0.80 | 0.71 |
| 15NC08 | | H | 0.010 | 3.80 | 0.010 | 0.12383 | 0.00014 | 0.83 | 0.81 |
| 15NC09 | | H | 0.090 | 2.02 | 0.211 | 0.12325 | 0.00014 | 1.76 | 0.89 |
| 15NC11 | Me Maoya massif | H | 0.010 | 1.76 | 0.030 | 0.13118 | 0.00018 | -0.24 | -0.22 |
| 15NC12 | | H | 0.030 | 1.09 | 0.128 | 0.12766 | 0.00035 | 0.39 | 0.27 |
| 15NC13 | | H | 0.010 | 0.02 | 1.275 | 0.13133 | 0.00144 | 0.12 | -0.24 |
| 15NC15 | | H | 0.001 | 0.05 | 0.162 | 0.12819 | 0.00069 | 0.32 | 0.20 |
| 15NC17 | | H | 0.010 | 3.45 | 0.018 | 0.12708 | 0.00020 | 0.37 | 0.36 |
| 15NC20 | | H | 0.001 | 0.02 | 0.205 | 0.12959 | 0.00084 | 0.00 | 0.00 |
| 15NC21 | | H | 0.010 | 0.39 | 0.148 | 0.12509 | 0.00032 | 0.98 | 0.64 |
| 15NC22 | | H | 0.001 | 0.03 | 0.346 | 0.12947 | 0.00113 | 0.10 | 0.02 |
| 15NC23 | | H | 0.020 | 0.30 | 0.315 | 0.12431 | 0.00054 | 2.86 | 0.75 |
| 15NC24 | | H | 0.001 | 0.03 | 0.345 | 0.13095 | 0.00085 | -1.04 | -0.19 |
| 15NC25 | | H | 0.200 | 1.62 | 0.586 | 0.12592 | 0.00022 | -1.37 | 0.52 |
| 15NC26 | | H | 0.001 | 0.06 | 0.141 | 0.12455 | 0.00079 | 1.06 | 0.71 |
| 15NC27 | | H | 0.010 | 1.07 | 0.028 | 0.12831 | 0.00028 | 0.20 | 0.18 |
| 15NC28 | | H | 0.020 | 1.73 | 0.045 | 0.12729 | 0.00030 | 0.37 | 0.33 |
| 15NC29 | | H | 0.001 | 0.84 | 0.001 | 0.12351 | 0.00028 | 0.86 | 0.86 |
| 15NC30 | | H | 0.001 | 0.24 | 0.048 | 0.12801 | 0.00095 | 0.25 | 0.22 |
| 15NC31 | | H | 0.010 | 0.70 | 0.047 | 0.12561 | 0.00029 | 0.63 | 0.56 |
| 15NC31-R | | H | 0.020 | 0.46 | 0.209 | 0.12594 | 0.00021 | 1.02 | 0.52 |
| 15NC32 | | H | 0.001 | 0.02 | 0.700 | 0.12762 | 0.00184 | -0.43 | 0.28 |
| 15NC33 | | H | 0.030 | 0.53 | 0.231 | 0.12557 | 0.00042 | 1.24 | 0.57 |
| 15NC34 | | H | 0.010 | 0.79 | 0.048 | 0.12565 | 0.00035 | 0.63 | 0.56 |
| 15NC37 | Tiebaghi massif | L | 0.17 | 3.62 | 0.226 | 0.12897 | 0.00015 | 0.19 | 0.09 |
| 15NC38 | | L | 0.27 | 3.99 | 0.326 | 0.12960 | 0.00014 | 0.00 | 0.00 |
| 15NC39 | | L | 0.38 | 4.02 | 0.456 | 0.12944 | 0.00016 | -0.30 | 0.02 |
| 15NC41 | | L | 0.38 | 3.80 | 0.484 | 0.12766 | 0.00022 | -1.95 | 0.27 |
| 15NC41-R | | L | 0.35 | 3.93 | 0.433 | 0.12750 | 0.00017 | -14.65 | 0.30 |
| 15NC42 | | L | 0.38 | 4.68 | 0.394 | 0.12898 | 0.00016 | 1.23 | 0.09 |
| 15NC43 | | L | 0.43 | 6.49 | 0.317 | 0.12843 | 0.00013 | 0.66 | 0.17 |
| 15NC44 | | L | 0.33 | 4.60 | 0.346 | 0.12857 | 0.00022 | 0.79 | 0.15 |
| 15NC45 | | L | 0.25 | 3.54 | 0.345 | 0.12956 | 0.00027 | 0.03 | 0.00 |
| 15NC46 | | L | 0.23 | 3.19 | 0.350 | 0.12387 | 0.00016 | 4.47 | 0.81 |
| 15NC48 | | L | 0.18 | 4.25 | 0.204 | 0.11990 | 0.00036 | 2.60 | 1.36 |

S: standards; H: harzburgites; L: lherzolites

R: replicate analysis

Both $T_{MA}$ and $T_{RD}$ are calculated relative to the primitive upper mantle, with parameters from Meisel et al. (2001).